Heliyon 9 (2023) e17136

Contents lists available at ScienceDirect

Heliyon

journal homepage: www.cell.com/heliyon

Development of gold plasmonic nanoparticles for detection of polydiallyldimethylammonium chloride at Umgeni water treatment plants: An optimised study and case application

Sabelo B. Mthembu [a], Damilola Caleb Akintayo [a,b,*], Brenda Moodley [a], Bhekumuzi P. Gumbi [a,**]

[a] School of Chemistry and Physics, University of KwaZulu-Natal, 54 University Road, Durban, 4001, South Africa
[b] University of Colorado, Aurora, CO, United States

ARTICLE INFO

Keywords:
AuNPs
Drinking water
Poly-(DADMAC)
Water treatment
UV–Vis spectrophotometry

ABSTRACT

Background: Polydiallyldimethylammonium chloride (poly-(DADMAC) is used in many drinking water treatment plants in most parts of the world as a flocculant to remove suspended solids from raw water. However, it is very important that residual poly-(DADMAC) is monitored because it disintegrates into a carcinogenic compound known as N-nitrosodimethylamine (NDMA) during the treatment of drinking water.

Methods: In this work, the gold nanoparticle method is optimised for the detection of poly-(DADMAC), where the gold nanoparticles were stabilised with trisodium citrate and then used in quantifying poly-(DADMAC) by Ultraviolet–Visible-Near Infrared spectrophotometry. The optimised method was able to measure poly-(DADMAC) at low concentrations of 1.000 μg L^{-1} in drinking water with limits of detection and limits of quantification of 0.3302 and 1.101 μg L^{-1}, respectively.

Significant results: The method was applied to two different water treatment plants and the concentration of poly-(DADMAC) found during stages of the water treatment process ranged from 1.013 to 33.63 μg L^{-1}. The average poly-(DADMAC) concentrate concentration that is dosed for coagulation in Umgeni Water plant A was 7.889 μg L^{-1} while in plant B was 19.28 μg L^{-1}. Residual poly-(DADMAC) concentration in drinking water was within the accepted limit of 50.00 μg L^{-1}, regulated by the World Health Organisation (WHO).

1. Introduction

The properties of gold, in its metallic state (redox state: 0), such as low reactivity towards sulphur (S), oxygen (O), concentrated acids, and bases are well understood, which makes it very important for human health applications such as dental and prostheses implants [1,2]. However, gold reacts completely in acidic solutions like aqua regia which has chlorine ions, and results in the formation of tetrachloroauric acid, $HAuCl_4$ (redox state of +3). Gold can also be biologically active when in solution and can be used to treat different cancers and rheumatic arthritis [3]. Sodium borohydride ($NaBH_4$) is normally used to reduce $HAuCl_4$ salt to gold

* Corresponding author. School of Chemistry and Physics, University of KwaZulu-Natal, 54 University Road, Durban, 4001, South Africa.
** Corresponding author.
E-mail addresses: damilola.akintayo@cuanschutz.edu (D.C. Akintayo), Gumbib@ukzn.ac.za (B.P. Gumbi).

https://doi.org/10.1016/j.heliyon.2023.e17136
Received 4 February 2023; Received in revised form 3 June 2023; Accepted 8 June 2023
Available online 9 June 2023

nanoparticles, and tri-sodium citrate ($Na_3C_6H_5O_7$) can be used both as a stabiliser or reducer at high temperatures. In this case, the gold nanoparticles, after reduction, have a metal redox state of 0.

Metal nanoparticles that contain noble elements such as platinum (Pt), silver (Ag), and gold (Au) have been employed in many studies for detection [3]. Among metal nanoparticles, gold nanoparticles (AuNPs) possess very unique and interesting optical properties. The metal nanoparticles have unique optical properties due to their large extinction coefficients. They are much more sensitive than organic probes and are therefore much more suitable for analysis. Hence, it is widely used in the determination of various analytes such as metal ions [4], proteins [5], small molecules [6], and anions [7]. They are much more sensitive than organic probes and are therefore much more suitable for analysis [3]. Gold nanoparticles undergo plasmon resonance, whereby the incident frequency of electromagnetic radiation experiences resonance with a delocalised electron cloud's oscillation. This localised surface plasmon resonates near the visible range for the gold nanoparticles, and because it is sensitive, it has been discovered that it can be [8] used as a probe to detect bio-molecules, organic molecules, and inorganic anions [9–15]. Colorimetric methods based on nanosensors are promising detectors for contaminants in the environment. They gained increasing attention because they are highly sensitive, and inexpensive and detection can be followed with the naked eye [16].

Cationic polyelectrolytes such as polydiallyldimethylammonium chloride (poly-(DADMAC)), acrylamide, and melanin-formaldehyde polymer are efficient in clarification of drinking water from dissolved and suspended materials [16]. Poly-(-DADMAC) is favoured as a flocculant because of its high charge density, which complements the progress of agglomeration of the suspended solids allowing it to easily settle the solids which are removed as sludge. It also aids in controlling algae and organic matter such as humic substances [16–19]. Recently, there is a growing concern about poly-(DADMAC)'s fate and toxicity in drinking water because its by-products such as N-nitrosoamine (NDMA) are reported to be carcinogenic [20–22]. Poly-(DADMAC) can still be present in low concentrations after the process of water treatment. Different methods have been used for detecting and quantifying poly-(-DADMAC) [23]. But the colorimetric probe-based gold nanoparticles method has an advantage over other analytical methods because it does not require many steps, it is efficient, and the colour change can be seen by the naked eye. Methods such as colloidal titration, metachromatic titration, viscometry and capillary electrophoresis have been investigated however they could not detect low concentrations ($\mu g\ L^{-1}$) [24]. Some of those methods which were able to detect low concentrations could not achieve great accuracy and precision and also required pre-treatment and lacked efficiency [23–26]. Methods developed for its quantification need to be able to detect poly-(DADMAC) at low concentrations. There is a need for a cheaper and simple method for routine analysis.

This study involves optimisation of a gold nanoparticle volume for routine monitoring of poly-(DADMAC) used in a drinking water treatment plant process. The optimised method was applied in monitoring samples from the drinking water treatment plant at different stages of the treatment process.

2. Experimental

2.1. Chemicals and reagents

Gold(III) chloride trihydrate ($HAuCl_4.3H_2O$) 99.9%, polydiallyldimethylammonium chloride ($C_8H_{16}ClN$) (poly-(DADMAC)), 35 wt.% (average molecular weight 100,000) and trisodium citrate ($Na_3C_6H_5O_7.2H_2O$) 99% were purchased from Merck (Sigma Aldrich (Hamburg, Germany)) and all were of analytical grade. Gradient Milli-Q (0.22 μm) Millipore water (18.2 $M\Omega\ cm^{-1}$ at 25 °C) was produced from our lab. There was no further purification was needed prior to the use of the chemicals.

2.2. Instrumentation

An Ocean Optics spectrometer (model HR2000+ manufactured by Ocean Optics at EW Duiven, Netherlands) was used to measure the absorbances and the data was acquired and analysed using Spectrasuite software (Ocean Optics, EW Duiven, Netherlands). A 1.0 cm quartz cuvette (Yixing Zhicheng Material Co., LTD., Jiangsu, China) was placed in the cuvette holder (Ocean Optics CUV-UV with a 1.0 cm path length bought from Ocean Optics at EW Duiven, Netherlands) and was used to measure sample absorbance. The light source used was a tungsten halogen (EW Duiven, Netherlands), (Ocean Optics) based module. The light traveled through a fiber optic cable, the cuvette holder, and finally through the second fiber optic cable (both cables were from Ocean Optics – 600-2-vis-BX model 727-733-2447 suitable for 400–2100 nm) to the spectrometer (EW Duiven, Netherlands). Characterisation of the gold nanoparticles was carried out using High-Resolution Transmission Electron Microscopy (HRTEM), a JEOL JEM-2100F transmission electron microscope (JEOL, Beijing, Shanghai, China).

2.3. Synthesis of gold nanoparticles

Gold nanoparticles were synthesised using a reduction method. An amount of 0.4866 g of gold(III) chloride trihydrate was dissolved in 400 mL Millipore water and heated on a hot plate up to 100 °C. A 10 mL solution of 0.2746 M trisodium citrate was poured into the boiling solution of gold salt with a continuous gentle stirring. The solution colour changed from yellow to a blackish colour and eventually to a deep red colour, which is the characteristic colour of gold nanoparticles normally used for analytical purposes which are between 20 nm and 40 nm.

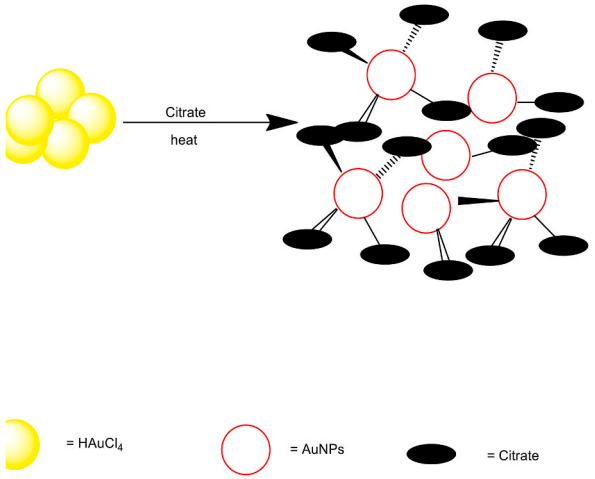

Fig. 1. Synthesis of gold nanoparticles [32]. (For interpretation of the references to colour in this figure legend, the reader is referred to the Web version of this article.)

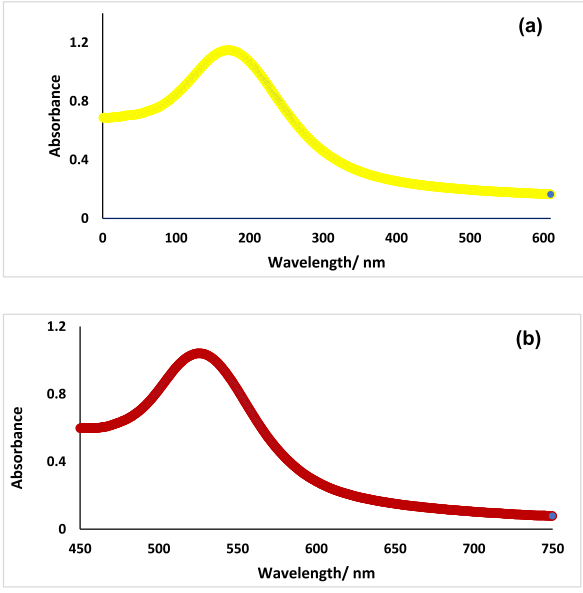

Fig. 2. UV–vis spectra of gold (III) salt (a) and gold nanoparticles (b). (For interpretation of the references to colour in this figure legend, the reader is referred to the Web version of this article.)

2.4. Preparation of poly-(DADMAC) stock and standards

A volume of 0.0542 mL of poly-(DADMAC) was transferred into a 1000 mL volumetric flask, filled up to the mark with Millipore water, and thoroughly shaken to ensure it was homogenised. The final concentration of the stock solution was 1750 μg L^{-1}. To make various poly-(DADMAC) concentrations of 1, 5, 10, 15, 20, 25 μg L^{-1}, volumes of 3, 14.3, 28.5, 42.9, 57 and 71 μL from the stock solution (1750 μg L^{-1}) were transferred into 5 mL volumetric flasks containing 2 mL of AuNPs solution and filled to the mark with Millipore water.

2.5. Characterisation of gold nanoparticles

To form nanoparticles, $AuCl_4^-$ was reduced by a reducing agent (citrate), and neutral gold atoms were produced (Au^{3+} to Au^0) [27]. The produced gold atoms undergo two processes which are nucleation and growth therefore forming gold nanoparticles capping agent ($C_3H_5O(CO_2)_3^{3-}$) presence stops the AuNPs from further nucleating and growing. There are many parameters contributing to the shape and size of AuNPs such as the temperature, rate of stirring, the mass of gold salt, and the speed at which the gold ions are reduced

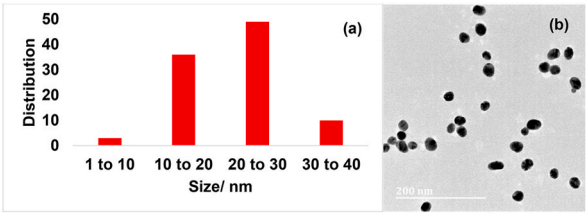

Fig. 3. Size distribution histogram (a) and TEM image of gold nanoparticles (b). (For interpretation of the references to colour in this figure legend, the reader is referred to the Web version of this article.)

Table 1
Average crystal sizes for AuNPs determined using PXRD.

2θ	D (nm)
31.69	1.501
35.29	0.3999
36.98	0.7310
38.03	0.2392
44.09	0.1644

[28–31]. Trisodium citrate played a dual role in the synthesis of AuNPs (Fig. 1), first, it reduces and then acts as a capping agent at 100 °C [29].

The synthesised nanoparticles were characterised using UV–Vis spectrophotometry. The UV–Vis spectrum of AuNPs in Fig. 2b depicts a new peak at wavelength 529 nm accompanied by a disappearance of a peak at 231 nm for the gold(III) salt (Fig. 2a). This shows that the absorbance peak of gold shifted to higher wavelengths when it was reduced and capped with citrate. This is known as surface plasmon resonance (SPR) [33]. It is important to note that the distance between the gold nanoparticles which are reciprocal, as well as their shape and size, affect this SPR. The SPR is around 529 nm for these synthesised gold nanoaparticles. This characteristic red colour is due to the distance between the gold nanoparticles, size, and an absorption overlapping between AuNPs [33]. This absorption is due to interband transitions such as an excitation of a single optical electron from a full 5 d band level to an empty 6s–6p band level of AuNPs [34]. The retardation effect happens because the multipolar plasmon modes become excited as the size of the AuNPs increases approaching the resonant electromagnetic wavelength. This phenomenon is electromagnetic, and it appears as a broadening and as a surface plasmon resonance red shift as the gold nanoparticle size increases and takes place at the optical absorption spectrum. The intensity of the surface plasmon resonance corresponds with the amount of AuNPs conduction electrons present, where an individual atom of gold contributes a single conducting electron [35]. This caters to their high extinction cross-section, which is ten thousand times bigger than that of organic chromophores.

The AuNPs were further analysed using High-Resolution Transmission Electron Microscopy (HRTEM) for imaging, which assists in determining the shape and size. From the TEM image (Fig. 3b), it can be observed that the AuNPs were scattered and spherical. The histogram in Fig. 3a shows the size distribution of the gold nanoparticles, with the majority of the AuNPs sizes ranging from 22 nm to 29 nm. Particle size distribution is a very significant factor in the application of gold nanoparticles. For this analysis particle sizes from 25 to 30 nm are desired to ensure the repeatability of the results.

Powder X-Ray diffraction (PXRD) cannot be used to determine the particle size because there is a difference between crystal and particle size. Crystal size is the size of crystals within the particle, it is very rare that the particle size is equal to the crystal size [36,37]. The Scherrer equation is normally used to determine the average crystal size [38].

The crystal size was calculated using the Scherrer equation (Eq. (1)).

$$D = \frac{K\lambda}{\beta \cos \theta} \tag{1}$$

where D represents the crystal size; K is the Scherrer constant (0.9); λ is the X-ray source wavelength, which is 0.15406 nm; β is the full width at half maximum (FWHM) in radians and lastly θ which is the peak position in radians. The obtained crystal sizes were tabulated below in Table 1.

When compared to the particle size of AuNPs, the crystal sizes of AuNPs are significantly smaller. The values were obtained from PXRD data and used in the Scherrer equation.

2.6. Gold nanoparticle poly-(DADMAC) complex characterisation

When poly-(DADMAC) was introduced into the AuNP solution, a plasmonic peak emerged at a higher wavelength around 650–690 nm. This is the product of plasmon hybridisation of particle aggregation, and this causes a colour change from red to blue in the AuNPs solution. The origins of plasmon resonance are in two bands; the first one is close to the original sphere's position and the second one is

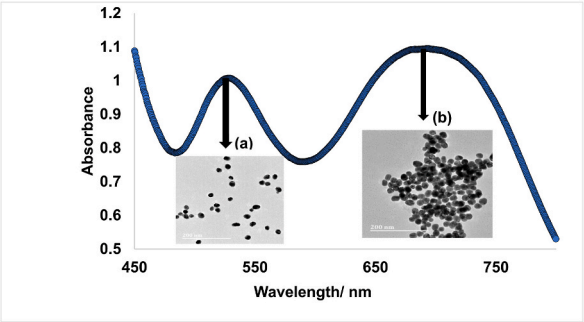

Fig. 4. UV–Vis spectrum of gold nanoparticles (a) and poly-(DADMAC)-AuNP complex (b). (For interpretation of the references to colour in this figure legend, the reader is referred to the Web version of this article.)

Table 2
Optimisation of volume of gold nanoparticles.

Volume of AuNPs/mL	Measured average poly-(DADMAC) concentration/μg L^{-1}	STDEV	Accuracy/ %	Precision/% RSD	% Error	LOD/μg L^{-1}	LOQ/μg L^{-1}	Equation/y = mx + c	R^2
5 mL volumetric flask									
1	0.2266	0.4724	22.66	208.5	77.34	3.240	10.80	0.0735x + 0.2288	0.9927
2	0.9557	0.0489	95.57	5.106	4.43	0.4917	1.600	0.0481x + 0.0867	0.9867
3	−1.157	0.0295	−115.7	2.548	215.7	0.8690	2.896	0.0274x + 0.1595	0.9905
10 mL volumetric flask									
2	0.1858	0.2055	18.58	110.6	81.42	0.3106	1.035	0.0862x + 0.2996	0.9755
4	0.9545	0.4762	95.45	49.89	4.55	5.675	18.92	0.0363x + 0.106	0.9942
6	−0.1540	0.2954	−15.40	−191.8	115.4	0.746	2.487	0.0335x + 0.1363	0.9975
20 mL volumetric flask									
4	3.425	0.3930	137.0	11.47	37.00	0.9743	3.248	0.0706x + 0.2051	0.9968
8	1.413	0.4550	56.52	32.19	54.35	1.366	4.555	0.025x + 0.0978	0.9695
12	0.9747	0.4077	38.99	41.38	61.01	1.257	4.190	0.0323x + 0.1441	0.9939

N = 3.

the red-shifted band (Fig. 4). This peak is due to the aggregation of AuNPs induced by poly-(DADMAC). Poly-(DADMAC) interacted with AuNPs in one of two scenarios; first, the poly-(DADMAC) replaces the citrate ions on the surface of the AuNPs surface, and the second scenario is that the poly-(DADMAC) surrounded the citrate ions. It is highly likely that the poly-(DADMAC) replaced the citrate ions due to the high affinity of AuNPs towards cationic molecules and nitrogen compared to citrate ions [13].

A colour change is observed when poly-(DADMAC) interacts with AuNPs, but small concentrations of poly-(DADMAC) from 0.5 to 5 μg L^{-1} did not show a significant change in colour. Poly-(DADMAC) concentrations greater than 10 μg L^{-1} caused a significant change in colour from deep red to blue occurs. This colour change was not due to the change in size or shape of the AuNPs but the plasmon shift to longer wavelengths as the formation of AuNP aggregation took place as confirmed by HRTEM [27]. Fig. 4b also demonstrates the TEM image of AuNPs complexed with poly-(DADMAC) and gives evidence that aggregation has taken place as the AuNPs were clustered while the AuNPs without poly-(DADMAC) were scattered (Fig. 4a).

3. Results and discussion

3.1. Optimisation of gold nanoparticle method

3.1.1. Volume of gold nanoparticles

To determine the concentration values for AuNPs using UV–Vis spectrophotometry, the obtained spectra which exhibited two peaks at wavelengths of 530 and 690 nm. The ratio ($\lambda_{690}/\lambda_{530}$) was use to obtain a calibration curve of various poly-(DADMAC). The calibration curve equation was then used to calculate the concentration of the analysed poly-(DADMAC) samples. Two parameters were optimised; the first was the volume of the volumetric flask and the second one was the concentration of AuNPs solution. Table 2

Table 3
Optimisation of gold nanoparticles concentration in a 5 mL volumetric flask.

AuNPs concentration/ (v/v)%	Poly-(DADMAC) concentration/μg L^{-1}	Measured Poly-(DADMAC) average concentration/μg L^{-1}	Accuracy/ %	Precision/% RSD	LOD/μg L^{-1}	LOQ/μg L^{-1}
20	1	0.2266	22.66	208.5	3.240	10.80
40	1	0.9557	95.57	5.106	0.4917	1.600
60	1	−1.157	−115.7	2.548	0.8690	2.896
20	2.5	2.040	81.60	1.912	3.240	10.80
40	2.5	0.2414	9.656	23.67	0.4917	1.600
60	2.5	−0.4680	−18.72	74.40	0.8690	2.896
20	5	5.673	113.5	7.911	3.240	10.80
40	5	5.461	109.5	17.32	0.4917	1.600
60	5	2.267	45.34	15.27	0.8690	2.896

N = 3.

Table 4
Intra-day and inter-day analysis obtained results for poly-(DADMAC).

Poly-(DADMAC) concentration/μg L^{-1}	Measured poly-(DADMAC) average concentration/μg L^{-1}	%Error	%RSD
Intra-day			
5	5.910 ± 0.088	18.0	1.489
40	42.53 ± 0.1239	5.06	0.2913
50	46.30 ± 06148	7.40	1.328
80	85.83 ± 0.9249	7.29	1.077
Inter-day			
5	5.592 ± 0.5840	11.84	10.44
40	41.69 ± 2.737	4.225	6.565
50	44.02 ± 2.263	11.96	5.141
80	86.38 ± 9.451	7.795	10.94

below shows an analysis of known concentrations of poly-(DADMAC) and varying calibration curves were used to obtain the actual concentrations by means of the equation of the straight line specific to each calibration curve. Accuracy was determined by dividing the concentration of the actual concentration over the known concentration. The standard deviation (STDEV) was used to determine how far the concentration values of poly-DADMAC are from each other. The lower the standard deviation, the more the concentration values are appreciated. Table 2 also shows Eq. (2) which is the detection limit (LOD), which gives an estimation about biasness and imprecision of the poly-DADMAC's low concentration levels, where σ is the standard deviation and S is the slope.

$$LOD = 3.3\sigma/S \quad (2)$$

$$LOQ = 10\sigma/S \quad (3)$$

Similarly, just like LOD the quantification limit (LOQ) which is Eq. (3) tells us the smallest concentration of poly-DADMAC that can be accurately measured using the optimised analytical procedure. It does not refer to the standard deviations of the blanks. The poly-(DADMAC) average concentration of 0.9557 μg L^{-1} obtained from the 5 mL volumetric flask displayed the best accuracy (95.57%) and was closest to the known concentration of 1.000 μg L^{-1} (accuracy), followed by 0.9545 μg L^{-1} from 10 mL with an accuracy of 95.45%. A poor accuracy (56.52%) was displayed by the obtained poly-(DADMAC) concentration of 1.413 μg L^{-1} from the volumetric flask of 20 mL, but it was not the poorest. The poorest accuracy was −15.40% and 18.48%. Gold nanoparticle solution of 2 mL in a 10 mL volumetric flask had the lowest LOD (0.3106) and LOQ (1.035 μg L^{-1}), exhibiting good sensitivity. However, it had accuracy of 18.58% and precision of 110.6% were not close to 100 and a % error of 81.42%. Comparing the volumetric flasks and the AuNPs solution volume, the 5 mL volumetric flasks showed best overall results it had a LOD of 0.4917 and LOQ of 1.600 μg L^{-1}.

3.1.2. Concentration of gold nanoparticles

Another parameter investigated was the concentration of the gold nanoparticles solution (v/v)%, which is the volume of the AuNPs over total solution's volume. A concentration of 20% (v/v) is obtained by transferring 1 mL of AuNPs in a 5 mL aqueous solution. Table 3 shows that the concentration of 40% gold nanoparticles solution is optimum for analysis. A AuNPs solution concentration of 40% in Table 3 gave a poly-(DADMAC) average concentration of 0.9557 μg L^{-1} with 95% accuracy, while other AuNPs concentrations were not accurate determining poly-(DADMAC) known concentration of 1 μg L^{-1} as prepared. Also, 40% AuNPs showed better accuracy compared to 20 and 60% AuNP with other known concentrations of 2.5 μg L^{-1} and 5.0 μg L^{-1}. The other methods either had a too high or too low concentration which was shown for both the 1 and 5 μg L^{-1} of poly-(DADMAC).

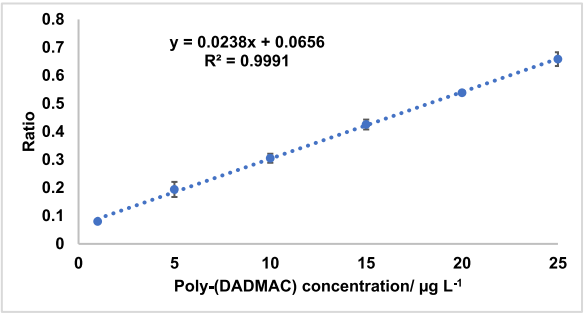

Fig. 5. Calibration curve of poly-(DADMAC) absorbance ratios at different concentrations (model).

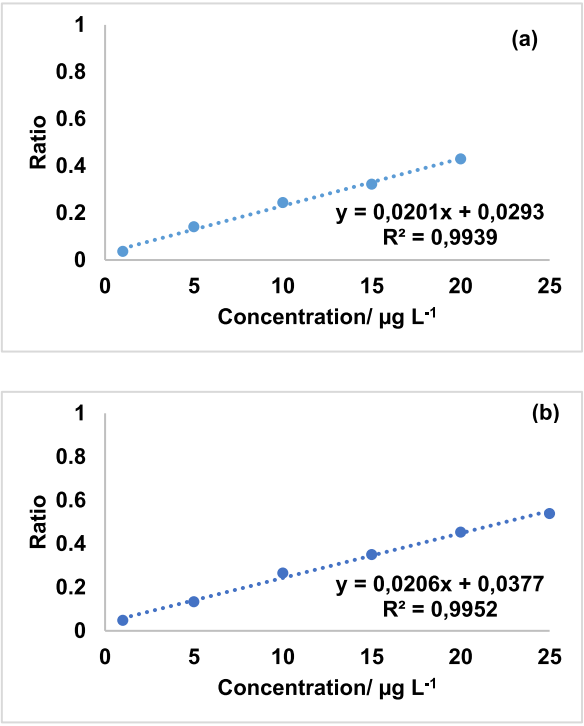

Fig. 6. Calibration curve of absorbance ratios at different concentrations of poly-(DADMAC) using raw water (a) and tap water (b).

3.2. Method validation

3.2.1. Precision

This study took place in one laboratory therefore repeatability is reported not reproducibility. However, intermediate precision is a good measure of the method when the routine analysis is desired. A triplicate of various sets of poly-(DADMAC) standards (5, 40, 50, and 80 µg L^{-1}) were prepared, and the inter-day and intra-day analyses were carried out to determine the intermediate precision of the method. The intra-day analysis was done on the same day but at different times and the inter-day analysis was done on different days, specifically for two days after the intra-day analysis but at the same times to mimic the monitoring routine in the plant. The obtained relative standard deviation (%RSD) of the results was the measurement of precision.

The results for intra-day and inter-day are presented in Table 4 which showed the %RSD was below 11%. This meant that the method had good precision. Intra-day analysis exhibited better %RSD values when compared to inter-day %RSD with values all below 2%, which indicate that this method is robust.

The calibration curve shown in Fig. 5 provided the detection limit of the method and the linearity. The absorbance ratio of absorbance peaks (690 nm/530 nm) was plotted against various poly-(DADMAC) concentrations. The gold nanoparticle solution's volume was 2 mL in a 5 mL volumetric flask (40% (v/v) for the preparation of standards. The external calibration curve was prepared using Millipore water.

Table 5
Detection limit.

LOD/μg L^{-1}	0.3302
LOQ μg L^{-1}	1.101
Linearity/μg L^{-1}	1–25
Equation	y = 0.0238x + 0.0656
R^2	0.9991
%RSD	3.29

Table 6
Data of matrix effect were the f and *t*-test was used.

Concentration (μg L^{-1})	F	T	Matrix effect
1	2.75	−3.40	No
5	8.01	1.96	No
10	1.44	−4.07	No
15	15.02	−6.15	No
20	3.35	−5.70	No

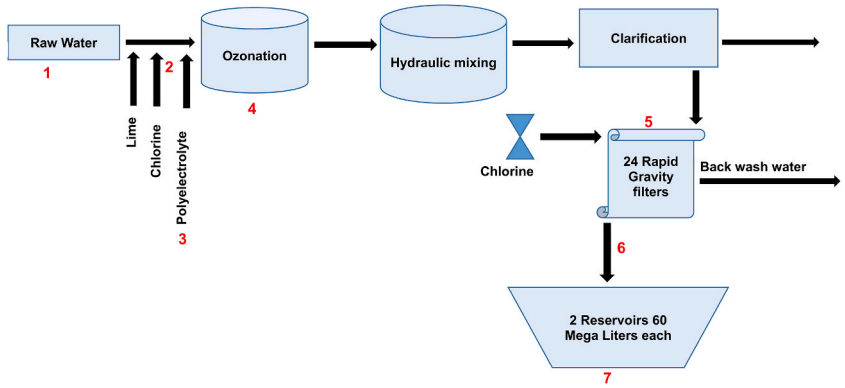

Fig. 7. Schematic flow diagram of water treatment process at Umgeni Water plant A water treatment plant showing the numbered sampling sites (1. Raw water, 2. After addition of chlorine, 3. Poly-(DADMAC) concentrate, 4 After addition of poly-(DADMAC), 5. Before sand bed, 6. After sand bed, 7. Reservoir, 8 Tap water).

3.2.2. Matrix match studies

To determine the effect of the matrix, two samples were collected at Umgeni Water treatment plant A. The first sample collected at the plant inlet was raw water coming from Inanda Dam, and the second sample was the effluent final tap water from the reservoir for distribution to the community. The raw water calibration curve was labeled Fig. 6a, and the second tap water calibration curve was labeled B Fig. 6b.

Both samples were spiked with various poly-(DADMAC) concentrations, ranging from 1 to 25 μg L^{-1} to construct a calibration curve and compare their calibration curves with the calibration curve of the model water (Millipore water). Table 5 was obtained when a calibration curve was made for model water and it showed good LOD and LOQ of 0.3302 and 1.101 μg L^{-1} respectively. It also had an acceptable %RSD of 3.29% which was below 10%.

When the above calibration curves (Figs. 5 and 6) were compared, they showed that the matrix effect can be neglected since the slopes of these calibration curves show no significant difference. Table 6 further confirms that through the use of f and *t*-test at a 95% confidence level which showed no significant difference in the values when the matrix effect was evaluated. This meant that raw water and tap water samples could be analysed using external calibration as there was no matrix effect and this method can be used as a routine method for monitoring poly-(DADMAC).

3.3. Application

The flow diagram in Fig. 7 shows Umgeni Water plant A drinking water treatment process. Umgeni Water treatment plant A is situated Wiggins, 6.8 km south west of Durban city centre in South Africa. About 350 mL of water are pumped from Inanda Dam per day which is used as a source of raw water to the plant for treatment. The raw water is chlorinated and ozonated and lime is added to balance the pH, after the addition of lime the polyelectrolytes are added to act as coagulants or flocculants. The polyelectrolytes used in these plants are a blend of poly-(DADMAC) and other polymers. The amount of polyelectrolyte dosed into the water after pH correction

Table 7
Poly-(DADMAC) blend concentration present in different water samples at various stages of the drinking water treatment process using the optimised method.

Water treatment stage	Week 1 poly-(DADMAC) sample concentration/μg L^{-1}	Week 2 poly-(DADMAC) sample concentration/μg L^{-1}	Week 3 poly-(DADMAC) sample concentration/μg L^{-1}
Tap water	–	0.6983 ± 0.082	3.462 ± 0.086
Raw water	2.675 ± 0.229	2.866 ± 0.178	3.683 ± 0.285
After addition of Chlorine	2.981 ± 0.302	3.513 ± 0.316	4.192 ± 0.095
After addition of poly-(DADMAC)	3.714 ± 0.370	5.564 ± 0.495	5.084 ± 0.111
Before sand bed	3.399 ± 0.486	2.172 ± 0.250	4.352 ± 0.151
After sand bed	2.717 ± 0.437	2.341 ± 0.139	4.647 ± 0.233
Reservoir	1.893 ± 0.315	1.342 ± 0.070	3.925 ± 0.129
Poly-(DADMAC) concentrate	6.948 ± 0.861	8.729 ± 1.08	7.990 ± 0.850

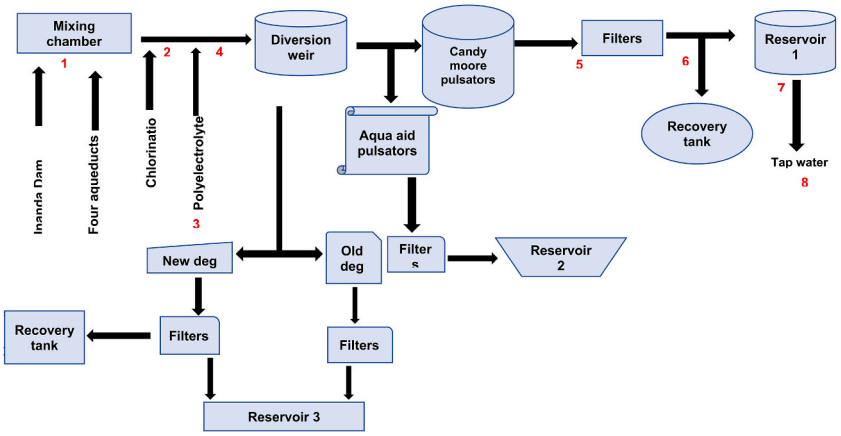

Fig. 8. Schematic presentation of Umgeni Water plant B water treatment process showing the numbered sampling sites (1. Raw water, 2. After addition of chlorine, 3. Poly-(DADMAC) concentrate, 4 After addition of poly-(DADMAC), 5. Before sand bed, 6. After sand bed, 7. Reservoir, 8 Tap water).

with lime differed based on the total dissolved solids in raw water. It was also noted that the polyelectrolyte is diluted to aid flow since polymers are vicious.

After the addition of poly-(DADMAC) and hydraulic mixing more chlorine was added. The 24 rapid filters are the sand bed filters through which the water passes to filter most of the solids. The sludge is carried away with backwash water and the filtered water goes to the reservoir. Water samples were collected during different stages of the drinking water process. The samples were collected from raw water, and after the second addition of chlorine where lime is first added to alter the pH of the water. Also, poly-(DADMAC) blend concentrate was collected, followed by the collection of the water sample after the addition of the poly-(DADMAC). Other sample points were before and after the sand bed gravity filtration and the final collection of samples was taken at the reservoir. This was done on Tuesdays from 11:30 a.m. to 12:00 p.m. for three consecutive weeks.

Water samples were collected at different stages of the drinking water treatment process at Umgeni Water plant A and they were analysed using optimised AuNPs UV–Vis spectrophotometry method. The information below shows the results obtained from the analysis.

Results presented in Table 7 shows that the amount of poly-(DADMAC) blend is below 5 μg L^{-1} which is the dosing concentration of the poly-(DADMAC) concentrate that is introduced into the treatment process. This concentration is much lower than the accepted amount of residual poly-(DADMAC) concentration of 10 μg L^{-1} determined by the World Health Organisation to be used as dosage [6]. Tap water obtained from Umgeni Water plant A water treatment plant at the drinking water treatment tap was analysed and it had a poly-(DADMAC) concentration of 0.6983 μg L^{-1} and 3.462 μg L^{-1} for week 2 and week 3, respectively.

Fig. 8 below shows the water treatment process at Umgeni Water plant B which is 17 km north west of Durban city centre in South Africa. The water samples were collected every Tuesday for 3 weeks. Raw water travels to the mixing chambers as raw water. After chlorination the polyelectrolyte (poly-(DADMAC) blend) is added to the water prior to the addition of lime, the water further travels to hydraulic flash mixers where it goes through a diversion weir. The diversion weir divides the water into four different streams, which are the candy moore plant, aqua aid, new deg, and old deg. Water from candy moore and aqua aid passes through pulsators and is filtered by sand beds. After filtration, it travels to the distribution chamber where it is divided into reservoir 1 and reservoir 2. Some of the water is recycled into recovery tank 1. Water from the new and old deg passes through pulsators to be filtered at the sand beds and

Table 8
Poly-(DADMAC) concentration during stages of the water treatment process at Umgeni Water plant B obtained using gold nanoparticle method recently optimised.

Water treatment stage	Week 1 poly-(DADMAC) sample concentration/μg L^{-1}	Week 2 poly-(DADMAC) sample concentration/μg L^{-1}	Week 3 poly-(DADMAC) sample concentration/μg L^{-1}
Tap water	1.456 ± 0.083	3.007 ± 0.315	1.192 ± 0.208
Raw water	2.096 ± 0.244	4.736 ± 0.618	4.514 ± 1.506
After addition of Chlorine	1.591 ± 0.117	2.431 ± 1.410	1.013 ± 0.365
After addition of poly-(DADMAC)	2.421 ± 0.068	2.249 ± 0.628	28.71 ± 0.775
Before sand bed	1.275 ± 0.051	2.444 ± 0.320	31.95 ± 1.418
After sand bed	1.409 ± 0.104	1.760 ± 0.143	1.195 ± 0.710
Reservoir	3.402 ± 0.072	2.462 ± 0.415	1.023 ± 0.011
Poly-(DADMAC) concentrate	4.010 ± 1.44	20.20 ± 4.38	33.63 ± 0.141

after chlorination, it is combined at the wet chamber and goes to reservoir 3. Some of the water is also recycled to recovery tank 2. Reservoir 1 stores 100 Mega litres of water, while reservoir 2 stores 43 Mega litres of water and most of the treated water is stored at reservoir 3 with a storage capacity of 346 Mega litres of water.

The results shown in Table 8 displayed below suggest that the amount of poly-(DADMAC) that has been introduced into the water treatment process increases with respect to the season. This may be due to the heavy rains this area experienced during the sampling, therefore more of the polymer is added proportionally with suspended solid. It was observed that the polymer concentrate dosing detected in the process rose from 4.010 to 33.63 μg L^{-1} from the beginning and end of the sampling. This trend is consistent with water after the addition of poly-(DADMAC) (2.421–28.71 μg L^{-1}) and water before the sand bed (1.275–31.95 μg L^{-1}) from week 1 to week 3. There was a difference in poly-(DADMAC) concentration between plant A and plant B, this is because both plants use different polymer blends with different percentage compositions which have different molecular weights.

4. Conclusion

The gold nanoparticles were successfully synthesised using gold(III) salt, reduced and stabilised at 100 °C. They were characterised using UV–Vis spectrophotometry and HRTEM. It was observed that majority of the nanoparticles ranged from 22 to 29 nm which was very close to the preferred range of 25–30 nm. The volume of the volumetric flask volume was optimised, and the best results obtained were found using the 5 mL volumetric flask. The concentration of the AuNPs solution in (v/v)% was also investigated. The AuNPs concentration that showed the best results was 40%, which was the most accurate and displayed low %RSD values. The LOD and LOQ of the chosen calibration curve based on accuracy and %RSD were 0.4917 and 1.600 μg L^{-1}, respectively.

From the inter and intra-day analysis it can be observed that the optimised gold nanoparticle method had good precision with all the %RSD values less than 11%. Water treatment plant A had poly-(DADMAC) concentrations below 5 μg L^{-1}, while plant B showed poly-(DADMAC) maximum concentrations which were much higher up to 31.95 μg L^{-1} but they were both lower than the accepted value stipulated by WHO. The application to real water samples shows the optimised method is suitable for different polymer blends. The calibration curve used to determine the poly-(DADMAC) concentration had a LOD and LOQ of 0.3302 and 1.101 μg L^{-1}. The optimised method will reduce the costs of the analysis by using lower concentrations of the gold nanoparticle solution at the same time improving the sensitivity of the method. Validation data support that this method is accurate and precise, and can be used for routine analysis of poly-(DADMAC).

Author contribution statement

Sabelo B Mthembu: Performed the experiments; Analysed and interpreted the data; Wrote the paper.

Damilola Caleb Akintayo: Conceived and designed the experiments; Wrote the paper.

Brenda Moodley, Bhekumuzi P Gumbi: Conceived and designed the experiments; Contributed reagents, materials, analysis tools or data; Wrote the paper.

Data availability statement

Data included in article/supp. material/referenced in article.

Declaration of competing interest

The authors declare that they have no known competing financial interests or personal relationships that could have appeared to influence the work reported in this paper.

Acknowledgements

We want to thank Umgeni Water for its financial support, which significantly contributed to this study. Also, National Research Foundation: Thuthuka grant holder linked bursary to grant number 122021.

References

[1] R. Doolabh, H.D. Dullabh, L.M. Sykes, A comparison of preload values in gold and titanium dental implant retaining screws, J. South Afr. Dent. Assoc. 69 (7) (2014) 316–320.
[2] M. Gjuric, S. Schagerl, Gold prostheses for ossiculoplasty, Am. J. Otol. 19 (3) (1998) 273–276.
[3] C.J. Murphy, et al., Gold nanoparticles in biology: beyond toxicity to cellular imaging, Acc. Chem. Res. 41 (12) (2008) 1721–1730.
[4] Y. Yu, et al., Mercaptosuccinic acid modified gold nanoparticles as colorimetric sensor for fast detection and simultaneous identification of Cr3+, Sens. Actuator, B: Chem. 239 (2017) 865–873.
[5] D. Kim, W.L. Daniel, C.A. Mirkin, Microarray-based multiplexed scanometric immunoassay for protein cancer markers using gold nanoparticle probes, Anal. Chem. 81 (21) (2009) 9183–9187.
[6] X. Esparza, et al., Hydrophilic interaction liquid chromatography/tandem mass spectrometry for the analysis of diallyldimethylammonium chloride in water, Rapid Commun. Mass Spectrom. 25 (2) (2011) 379–386.
[7] B. Amanulla, et al., Selective colorimetric detection of nitrite in water using chitosan stabilized gold nanoparticles decorated reduced graphene oxide, Sci. Rep. 7 (14182) (2017) 1–9.
[8] R. Rojas-Reyna, et al., Flocculation efficiency of modified water soluble chitosan versus commonly used commercial polyelectrolytes, Carbohydr. Polym. 81 (2) (2010) 317–322.
[9] S.K. Menon, et al., Analytical detection and method development of anticancer drug Gemcitabine HCl using gold nanoparticles, Spectrochim. Acta, Part A 94 (2012) 235–242.
[10] P.C. Ray, Size and shape dependent second order nonlinear optical properties of nanomaterials and their application in biological and chemical sensing, Chem. Rev. 110 (9) (2010) 5332–5365.
[11] D. Vilela, M.C. Gonzalez, A. Escarpa, Sensing colorimetric approaches based on gold and silver nanoparticles aggregation: chemical creativity behind the assay A review, Anal. Chim. Acta 751 (2012) 24–43.
[12] Z. Wang, L. Ma, Gold nanoparticle probes, Coord. Chem. Rev. 253 (11) (2009) 1607–1618.
[13] W. Liu, et al., A highly sensitive, dual-readout assay based on gold nanoparticles for organophosphorus and carbamate pesticides, Anal. Chem. 84 (9) (2012) 4185–4191.
[14] Z.Q. Tan, J.F. Liu, Visual test of subparts per billion-level mercuric ion with a gold nanoparticle probe after preconcentration by hollow fiber supported liquid membrane, Anal. Chem. 82 (10) (2010) 4222–4228.
[15] M.A. Yukselen, J. Gregory, The reversibility of floc breakage, Int. J. Miner. Process. 73 (2) (2004) 251–259.
[16] K. Sang-kyu, G. John, Charge determination of synthetic cationic polyelectrolytes by colloidal titration, Colloids Surf., A 159 (1) (1999) 165–179.
[17] J. Yu, et al., Flocculation of kaolin particles by two typical polyelectrolytes: a comparative study on the kinetics and floc structures, Colloids Surf. A Physicochem. Eng. Asp. 290 (1) (2006) 288–294.
[18] B. Tian, et al., Adsorption and flocculation behaviors of polydiallyldimethylammonium (PDADMA) salts: influence of counterion, Int. J. Miner. Process. 79 (4) (2006) 209–216.
[19] R. Greenwood, K. Kendall, Effect of ionic strength on the adsorption of cationic polyelectrolytes onto alumina studied using electroacoustic measurements, Powder Technol. 113 (1) (2000) 148–157.
[20] J. Choi, R.L. Valentine, Formation of N-nitrosodimethylamine (NDMA) from reaction of monochloramine: a new disinfection by-product, Water Res. 36 (4) (2002) 817–824.
[21] S.E. Magubane, et al., Optimization of CIEL*a*b*/Yxy colour system for colorimetric devices fabricated with gold nanoparticles, J. Mol. Struct. 1191 (2019) 271–277.
[22] S. Majam, P.A. Thompson, Polyelectrolyte determination in drinking water, Water SA 32 (5) (2006) 705–707.
[23] I.W. Mwangi, et al., Method development for the determination of diallyldimethylammonium chloride at trace levels by epoxidation process, Water, Air, Soil Pollut. 224 (9) (2013) 1638.
[24] B. Gumbi, J.C. Ngila, P.G. Ndungu, Gold nanoparticles for the quantification of very low levels of poly-diallyldimethylammonium chloride in river water, Anal. Methods 6 (17) (2014) 6963–6972.
[25] G. Marcelo, M.P. Tarazona, E. Saiz, Solution properties of poly(diallyldimethylammonium chloride) (PDDA), Polymer 46 (8) (2005) 2584–2594.
[26] N. Anik, et al., Characterization of cationic copolymers by capillary electrophoresis using indirect UV detection and contactless conductivity detection, J. Chromatogr. A 1219 (2012) 188–194.
[27] H.W. Cheng, et al., Chapter 2-Synthesis of gold nanoparticles, Compr. Anal. Chem. 66 (1) (2014) 37–79.
[28] K.R. Brown, D.G. Walter, M.J. Natan, Seeding of colloidal Au nanoparticle solutions. 2. Improved control of particle size and shape, Chem. Mater. 12 (2) (2000) 306–313.
[29] D.T. Nguyen, D.J. Kim, K.S. Kim, Controlled synthesis and biomolecular probe application of gold nanoparticles, Micron 42 (3) (2011).
[30] K. Saha, et al., Gold nanoparticles in chemical and biological sensing, Chem. Rev. 112 (5) (2012) 2739–2779.
[31] E.C. Dreaden, et al., The golden age: gold nanoparticles for biomedicine, Chem. Soc. Rev. 41 (7) (2012) 2740–2779.
[32] H.W. Cheng, et al., Chapter 2-synthesis of AuNPs, Compr. Anal. Chem. 66 (2014).
[33] M.J.A. Parra, S.S. Paradinas, Spectroscopic techniques based on the use of gold nanoparticles, Compr. Anal. Chem. 66 (2014) 477–527.
[34] U. Kreibig, M. Vollmer, Optical Properties of Metal Clusters, vol. 25, Springer, 1995, p. 535.
[35] V. Amendola, M. Meneghetti, Size evaluation of gold nanoparticles by UV−Vis spectroscopy, J. Phys. Chem. B 113 (11) (2009) 4277–4285.
[36] K. He, et al., Method for determining crystal grain size by X-ray diffraction, Cryst. Res. Technol. 53 (2) (2018), 1700157.
[37] P. Wang, et al., High (111) orientation poly-Ge film fabricated by Al induced crystallization without the introduction of AlOx interlayer, Mater. Res. Bull. 72 (2015) 60–63.
[38] S. Fayazzadeh, M. Khodaei, Salt-assisted combustion synthesis of cobalt ferrite nanoparticles; magnetic properties and cation distribution measurement by XRD analysis, J. Ultrafine Grained Nanostruct. Mater. 52 (1) (2019) 69–77.